Expression of the circadian clock gene *Period2* in the hippocampus: possible implications for synaptic plasticity and learned behaviour

Louisa M–C Wang*,†, Joanna M Dragich*,†, Takashi Kudo*, Irene H Odom*, David K Welsh‡,§, Thomas J O'Dell‖ and Christopher S Colwell*1

*Department of Psychiatry and Biobehavioral Sciences, University of California, Los Angeles, 760 Westwood Plaza, Los Angeles, CA 90024-1759, U.S.A.
†Department of Neurology, Columbia University, New York City, NY 10032, U.S.A.
‡Departmentof Psychiatry and Cell and Developmental Biology, University of California, San Diego, La Jolla, CA 92093, U.S.A.
§Veterans Affairs San Diego Healthcare System, San Diego, CA 92161, U.S.A.
‖Department of Physiology, University of California, Los Angeles, 760 Westwood Plaza, Los Angeles, CA 90024-1759, U.S.A.

ABSTRACT

Genes responsible for generating circadian oscillations are expressed in a variety of brain regions not typically associated with circadian timing. The functions of this clock gene expression are largely unknown, and in the present study we sought to explore the role of the *Per2* (Period 2) gene in hippocampal physiology and learned behaviour. We found that PER2 protein is highly expressed in hippocampal pyramidal cell layers and that the expression of both protein and mRNA varies with a circadian rhythm. The peaks of these rhythms occur in the late night or early morning and are almost 180° out-of-phase with the expression rhythms measured from the suprachiasmatic nucleus of the same animals. The rhythms in *Per2* expression are autonomous as they are present in isolated hippocampal slices maintained in culture. Physiologically, *Per2*-mutant mice exhibit abnormal long-term potentiation. The underlying mechanism is suggested by the finding that levels of phosphorylated cAMP-response-element-binding protein, but not phosphorylated extracellular-signal-regulated kinase, are reduced in hippocampal tissue from mutant mice. Finally, *Per2*-mutant mice exhibit deficits in the recall of trace, but not cued, fear conditioning. Taken together, these results provide evidence that hippocampal cells contain an autonomous circadian clock. Furthermore, the clock gene *Per2* may play a role in the regulation of long-term potentiation and in the recall of some forms of learned behaviour.

Key words: circadian rhythm, fear conditioning, hippocampus, long-term potentiation, memory, Period 2.

INTRODUCTION

A variety of studies suggest that learning and memory processes are sensitive to disruptions in sleep and circadian rhythms (Dijk et al., 1992; Peigneux et al., 2004; Ellenbogen et al., 2006; Wright et al., 2006; Ruby et al., 2008). The circadian system can also influence the acquisition and recall of learned behaviours (Valentinuzzi et al., 2001; Chaudhury and Colwell, 2002; Fernandez et al., 2003; Lyons et al., 2006; Eckel-Mahan et al., 2008). Mutations in at least some of the genes responsible for the generation of circadian oscillations can alter learning in mice (Garcia et al., 2000; Abarca et al., 2002; Hampp et al., 2008) and *Drosophila* (Sakai et al., 2004). Mechanistically, similar sets of cellular and molecular processes are thought to underlie both circadian oscillations and behavioural plasticity. For example, specific transcription factors play a critical role in both the regulation of circadian rhythms (Gau et al., 2002; Reppert and Weaver, 2002) and in at least some forms of learned behaviours (Kandel, 2001;

Bozon et al., 2003). These types of observations suggest that there may be a fundamental interaction between learning and memory processes and the circadian system.

In mammals, neurons responsible for the generation and co-ordination of circadian rhythms are located in the SCN (suprachiasmatic nucleus) in the hypothalamus. These cells possess anatomical, physiological and molecular specializations that allow them to perform these functions. At the molecular level, a set of interacting transcriptional/translational feedback loops are responsible for the generation of these circadian oscillations (Reppert and Weaver, 2002; Ko and Takahashi, 2006). One of the key genes involved in this molecular timing system is the *Period2* gene (*Per2*). Mutations in *Per2* shorten the fundamental frequency of circadian oscillations and cause the eventual loss of behavioural rhythms (Zheng et al., 1999; Bae et al., 2001; Xu et al., 2007). In humans, mutations in *hPer2* (human *Per2*) are associated with alterations in the timing of the sleep/wake cycle (Toh et al., 2001; Vanselow et al., 2006; Xu et al., 2007).

Previous evidence demonstrates that clock genes, including *Per2*, are widely expressed in peripheral organs as well as in the nervous system (Abe et al., 2002; Yoo et al., 2004). In mammals, these circadian-related genes are found in brain regions critical to learned behaviours including the hippocampus (Wakamatsu et al., 2001; Lamont et al., 2005; Chaudhury et al., 2008), the amygdala (Lamont et al., 2005) and the ventral tegmental area (McClung et al., 2005). The functions served by these genes outside of the SCN are just beginning to be examined. Therefore, in the present study, we started with the careful description of the circadian regulation of levels of *Per2* mRNA and protein in the hippocampus and SCN of the same animals. We then used an optical reporter of PER expression in order to determine whether the circadian rhythm could be measured in the isolated hippocampus. Finally, the presence of *Per2* in the hippocampus, and the rich literature implicating this structure in learned behaviours (Squire, 1992), led us to carry out a set of experiments designed to explore the role of *Per2* in hippocampal physiology and learned behaviour.

MATERIALS AND METHODS

Animals

In all studies, we followed guidelines from the National Institutes of Health, and regulations for animal use prescribed by the UCLA (University of California, Los Angeles) Division of Laboratory Animals or the Committee on Animal Care and Use at The Scripps Research Institute. For the gene expression studies, we obtained C57 Bl/6 mice from breeding colonies at UCLA. Animals in the day group were placed in chambers where lights were on at 07:00 hours and off at 19:00 hours.

Animals in the night group were placed in a reversed LD (light/dark) cycle where lights were on at 22:00 hours and off at 10:00 hours. These mice are placed in this reversed LD cycle upon weaning at 14–21 days of age and were then maintained on this LD cycle until they were used in the experiments at 4–6 months of age. For analysis of locomotor activity patterns, male mice were housed individually and their wheel-running activity recorded as revolutions per 3 min intervals. The running wheels and data acquisition systems were obtained from the Mini Mitter Company. The animals were exposed to a 12 h/12 h LD cycle for 2–3 weeks, and then placed into constant darkness (termed DD) for 2 weeks prior to assessing their free-running activity pattern. All handling of animals was carried out either in the light portion of the LD cycle or in DD with the aid of an IR viewer (Night Optics).

Male *Per2*-mutant (Zheng et al., 1999) and age-matched WT (wild-type) mice were obtained from Jackson Laboratories. The mice were genotyped at Jackson Laboratories prior to shipment to UCLA. The *Per2*-mutant mice contain a point mutation (G-to-T transversion) in the *Per2* gene that leads to the generation of PER2 protein containing an 87-amino-acid deletion. These mice were backcrossed for 5–6 generations into the C57 line and thus are 96.9–98.4% C57 Bl/6. More information on these *Per2*-mutant mice can be found at http://www.informatics.jax.org. Animals in the day group were placed in chambers where lights were on at 07:00 hours and off at 19:00 hours. Animals in the night group were placed in a reversed LD cycle where lights were on at 22:00 hours and off at 10:00 hours. Animals were allowed to entrain to the LD cycle for at least 2 months prior to experimentation. For analysis of locomotor activity patterns, male mice were housed individually and their wheel-running activity recorded as revolutions per 3 min intervals. The running wheels and data acquisition systems were obtained from the Mini Mitter Company.

For bioluminescence imaging experiments, we used both *Per2*::LUC and *Per2*::LUC-SV40 mice. In these knockin mice, the endogenous *Per2* gene is replaced by a fusion of *Per2* and the firefly luciferase gene (*luc*+), such that an *Per2*::LUC fusion protein is expressed, reflecting both transcriptional and post-transcriptional regulation of the *Per2* locus (Yoo et al., 2004; Welsh et al., 2004, 2005). The two strains are identical, except that the targeting construct for the *Per2*::LUC-SV40 strain contains an SV40 polyadenylation site after luciferase, resulting in ~30% brighter luminescence in cultured cells (DK Welsh, unpublished data).

IHC (immunohistochemistry)

Mice were anaesthetized and perfused with PBS followed by 4% (w/v) paraformaldehyde in PBS. Brains were dissected, post-fixed at 4°C overnight, and cryoprotected in 30% sucrose in PBS. IHC was performed on free-floating 30 μm cryostat coronal brain sections of C57 mice. Sections were washed for 5 min with PBS (twice), then incubated in 2%

H₂O₂ in PBS (10 min). Sections were then washed again in PBS (three times), dipped in 10% normal goat serum in PBS for 2 h, and then incubated with a 1:1000 dilution of rabbit anti-PER2 antiserum (Alpha Diagnostics) in PBS at 4°C overnight. Sections were washed in PBS (three times), then incubated with biotinylated goat anti-rabbit antibody at 1:2000 for 2 h. Sections were washed again for 10 min in PBS (three times) and dipped in AB solution (Vector Labortories) for 1 h, washed again in PBS, then placed in filtered 0.05% 3,3′-diaminobenzidine in PBS containing a 1:10000 dilution of 30% H₂O₂. After sufficient colour reaction (2–3 min), sections were washed with PBS and mounted on slides immediately. Sections were then dried overnight, washed with water for 10 min, dehydrated with ascending concentrations of ethanol, and cover-slipped. Images were captured with Axio Vision camera systems (Carl Zeiss). Blocking experiments, performed by adding the PER2 peptide (1 mg/ml in PBS, pH 7.4, diluted 1:500) to the primary incubation solution, prevented PER2 staining. A fixed brain from a *Per2*-null mouse (Per2KO#6128) was provided by Dr David Weaver (University of Massachusetts Medical School, Worcester, MA, U.S.A.).

We defined the hippocampus [CA1 (where CA is cornu ammonis), CA2, CA3, DG (dentate gyrus)] and SCN by using Cresyl-Violet-stained mouse brains as a reference. For each mouse, images were captured from each of these three regions using a SPOT camera system (Diagnostic Instruments). Three tissue sections from each region (CA1, CA2, CA3 and DG) were chosen at random and images taken. The representative sections were obtained from at least three animals. All immunopositive cells within the hippocampus and SCN of these regions were counted manually at 400× with the aid of a grid (200 μm × 400 μm). All immunopositive cells within the grid were counted equally without regard to the intensity of the staining. Counts were performed by two observers blinded to the treatment protocol and the results were averaged.

For fluorescence IHC, mice were anaesthetized and perfused with PBS followed by 4% (w/v) paraformaldehyde in PBS. Brains were dissected, post-fixed at 4°C overnight, and cryoprotected in 20% sucrose in PBS. Fluorescence IHC was performed simultaneously on free-floating 20-μm cryostat coronal brain sections of mice. Sections were washed for 10 min with PBS. Sections were dipped in 3% normal goat serum in PBS with 0.1% Triton X-100 for 1 h, and then incubated with an affinity-purified rabbit polyclonal antibody raised against PER2 (Alpha Diagnostics; #PER21-A) diluted 1:2000 with a solution of Triton X-100/PBS with 3% normal goat serum. Sections were incubated with the primary antibody for 72 h at 4°C. Sections were rinsed in PBS and incubated for 2 h with an Alexa Fluor® 488 goat anti-rabbit IgG (Invitrogen), diluted 1:200 with Triton X-100/PBS with 3% normal goat serum. Next, sections were washed with PBS and incubated for 10 min with TO-PRO3 (Invitrogen), diluted 1:500 with PBS. After incubation, sections were rinsed in PBS and immediately mounted on slides. Sections were then dried and coverslipped. Then, sections were imaged on the Zeiss Axiovert 200M microscope with an attached Zeiss LSM 510 META laser-scanning confocal microscope system.

Western blot analysis

Whole hippocampus was flash frozen in 500 μl of ice-cold homogenization buffer [50 mM Tris/HCl (pH 7.0), 50 mM NaF, 10 mM EGTA, 10 mM EDTA, 80 μM sodium molybdate, 5 mM sodium pyrophosphate, 1 mM sodium orthovanadate, 0.01% Triton X-100 and 4 mM *p*-nitrophenylphosphate]. The homogenization buffer also contained cocktails of protease inhibitors (Protease Inhibitors Complete; Roche Molecular Biochemicals) and protein phosphatase inhibitors (Protein Phosphatase Inhibitor Cocktail I and II; Sigma–Aldrich). The tissue was homogenized with an ultrasonic cell disruptor (three times for 5 s each). Immediately after homogenization, aliquots were removed for protein analysis, and equal amounts of denaturing protein loading buffer [0.5 M Tris/HCl (pH 6.8), 4.4% (w/v) SDS, 20% (v/v) glycerol, 2% 2-mercaptoethanol and Bromophenol Blue] were added. These homogenates were kept on ice for ~45 min while protein concentrations were determined using a Bio-Rad Protein Assay Kit. Homogenates containing 20–30 μg of protein each were electrophoresed on SDS/PAGE (15% gels), transferred on to nitrocellulose membranes, and probed with various primary anti-sera (1:1000) overnight [PER2 (Alpha Diagnostics), tubulin, p-ERK (phosphorylated extracellular-signal-regulated kinase), total ERK, p-CREB (phosphorylated cAMP-response-element-binding protein) and total CREB (all from Millipore). The membranes were incubated with HRP (horseradish peroxidase)-conjugated anti-mouse or anti-rabbit secondary IgG (1:1000), and protein signals were visualized by chemiluminescence (Immun-Star HRP detection kit; Bio-Rad). A phosphorimager was used for quantification, and day/night comparisons were analysed simultaneously, using identical settings. Protein bands were boxed, and the integrated intensity of all the pixels within that band was calculated above object average background levels of a box of the same size. Percentage changes attributable to temporal variation were calculated relative to the absorbance of the corresponding untreated protein bands within a single experiment, and Student's *t* tests were used to assess statistical significance. To quantify changes in p-ERK compared with total ERK or p-CREB compared with total CREB protein expression, protein from the same hippocampal samples were run simultaneously and probed with either p-ERK or total ERK and p-CREB or total CREB. To control for potential variations in loading, the absorbance of bands for each protein of interest were first normalized to the absorbance values obtained for tubulin loading control bands in each lane. Tubulin absorbance values did not vary as a function of time when mice were held in an LD cycle [ZT (zeitgeber time) 2: 1308±90; ZT 6: 1330±64; ZT 10: 1322±126; ZT 14: 1293±21; ZT 18: 1400±51; ZT 22: 1345±113] or in DD [CT (circadian time) 2: 1475±34; CT 6:

1521 $\pm$ 51; CT 10: 1663 $\pm$ 59; CT 14: 1547 $\pm$ 130; CT 18: 1674 $\pm$ 162; CT 22: 1635 $\pm$ 110]. In some cases, normalized values were then expressed as a percentage of the levels seen in control (day) samples or as a ratio of phospho/total ERK or CREB protein expression.

ISH (*in situ* hybridization)

A plasmid (pCRII; Invitrogen) containing the cDNA for *Per2* (nucleotides 9–489, accession number AF035830) was provided by Dr David Weaver (University of Massachusetts Medical School, Worcester, MA, U.S.A.) and insert identity was confirmed by sequencing using the M13R primer. To generate antisense and sense templates for ISH, plasmids were linearized overnight, phenol/chloroform extracted, ethanol precipitated and resuspended in DEPC (diethyl pyrocarbonate)-treated water. Riboprobes were synthesized from 1 μg of template cDNA in a reaction mixture containing 100 mCi of [^{35}S]UTP (1250 Ci/mmol; PerkinElmer), 5 $\times$ transcription buffer (Promega), 0.1 M DTT (dithiothreitol; Promega), 10 mM of each rATP, rCTP and rGTP, 40 units of RNase inhibitor, and the appropriate RNA transcriptase (SP6 or T7), for 3 h at 37°C. The *in vitro* transcription reaction was DNase I treated, and then unincorporated nucleotides were removed using RNase-free microfuge spin columns (Bio-Spin 30; Bio-Rad) and probe yields were calculated by scintillation counting. ISH on tissue sections was performed using previously described procedures (Lambert et al., 2005; Chaudhury et al., 2008). Briefly, tissue sections were fixed in 4% (w/v) paraformaldehyde, air-dried and blocked by acetylation with acetic anhydride, followed by a series of dehydration steps. After air drying, slides were placed in pre-hybridization buffer [50% formamide, 3 M NaCl, 20 mM EDTA, 400 mM Tris (pH 7.8), 0.4% SDS, 2 $\times$ Denhardt's (0.02% Ficoll 400/0.02% polyvinylpyrrolidone/0.02% BSA), 500 mg/ml tRNA and 50 mg/ml poly(A)$^{+}$ RNA (polyadenylated RNA)] for 1 h at 55°C. Sections were hybridized overnight at 55°C in humidified chambers in hybridization buffer [50% formamide, 10% dextran sulfate, 3 M NaCl, 20 mM EDTA, 400 mM Tris (pH 7.8), 0.4% SDS, 2 $\times$ Denhardt's, 500 mg/ml tRNA, 50 mg/ml poly(A)$^{+}$ RNA and 40 mM DTT], where each slide was incubated with 1–4 $\times$ 10^{6} c.p.m./70 ml of a riboprobe. All post-hybridization washes contained 1 mM sodium thiosulfate, except in the RNase A and ethanol washes. Following hybridization, the slides were washed for 15 min in 4 $\times$ SSC (1 $\times$ SSC is 0.15 M NaCl/0.015 M sodium citrate), at their respective hybridization temperatures, in 2 $\times$ SSC for 1 h at room temperature (25°C), and then RNase A (20 mg/ml) treated at 37°C for 30 min to remove unbound probe. To further reduce non-specific hybridization, the slides were washed twice in 2 $\times$ SSC at 37°C, and for 1 h in 0.1 $\times$ SSC at 62–67°C. Slides were serially dehydrated in ethanol containing 0.3 M ammonium acetate and exposed to Kodak Biomax MR film (Kodak) along with a ^{14}C slide standard (American Radiolabeled Chemicals). Following the initial exposure, the slides were emulsion-dipped (NTB;

Kodak), dried and stored in a desiccated, lightproof container for 14 days. Emulsion-dipped sections were developed in D19 developer (Kodak), fixed (Fixer; Kodak), and then counterstained with 0.04% Thionin dye to serve as a reference. Densitometric analysis of hybridization intensity was performed as described using NIH (National Institutes of Health) image software (Shearman et al., 1997; Chaudhury et al., 2008).

Brain slice culture

Hippocampal and cerebellar slices were obtained from 4- to 5-day-old mice in a colony maintained on an LD cycle (12 h/ 12 h, with lights on at 07:00 hours). Dissections were performed at mid-day, during the light portion of the LD cycle. Hippocampi were separated manually from 400 μm coronal brain slices, including a small portion of cingulate cortex. Slices were cultured in Hepes-buffered, air-equilibrated DMEM (Dulbecco's modified Eagle's medium; GIBCO 12100-046, Invitrogen) supplemented with 1.2 g/l NaHCO$_3$, 10 mM Hepes, 4 mM glutamine, 25 units/ml penicillin, 25 μg/ml streptomycin, 2% B-27 (GIBCO 17504-044) and 1 mM luciferin (BioSynth). Each brain slice was cultured on a Millicell-CM membrane insert (Fisher PICMORG50), and placed in a 35-mm culture dish containing 1 ml of medium. The dish was covered by a 40-mm circular coverslip (Erie Scientific), sealed in place with vacuum grease to prevent evaporation.

Measurement of bioluminescence

To monitor circadian rhythms of bioluminescence, we placed the dishes in a luminometer (Actimetrics) which fitted inside a standard tissue culture incubator kept at 36°C, 0% CO$_2$. Luminescence from each dish was measured by a photomultiplier tube for ~70 s at intervals of 10 min. For imaging of bioluminescence, one dish was sealed and placed on the stage of an inverted microscope (Olympus IX70). A heated lucite chamber around the microscope stage (Solent Scientific) kept the cells at a constant temperature of 36°C. Light was collected using an Olympus 4 $\times$ UPlanApo objective (NA 0.16) and transmitted to a CCD (charge-coupled-device) camera (Spectral Instruments SI800) cooled to −90°C. Images of 29.5 min exposure duration were collected at 30 min intervals for 12 days (Welsh et al., 2004, 2005).

Bioluminescence image processing and analysis

In MetaMorph (Molecular Devices), cosmic ray artifacts were removed by using the minimum value in a pixelwise comparison of consecutive images. Thus, pixel data were effectively smoothed by a running minimum algorithm, with a 1 h temporal window. Images were corrected for bias and dark current by background subtraction. In the resulting stack of images, luminescence intensity was measured within a region of interest defined manually. The position of a region

was adjusted if necessary to accommodate movements of cells. Data were logged to Microsoft Excel for further processing and plotting. Luminescence intensity values were converted into photons/min based on the rated quantum efficiency and gain of the camera.

Luminescence time series were imported into Lumicycle Analysis (Actimetrics) for rhythm analysis. In some experiments we observed high initial transients of luminescence, and therefore we excluded the first 12 h of data from rhythm analysis. A linear baseline (polynomial order=1) was subtracted from the data, and the subtracted data were then fitted to a sine wave with exponentially decaying amplitude (Welsh et al., 2004). Period was defined as the period of the best-fit sine wave.

Field potential electrophysiology

Methods were as previously described (Chaudhury et al., 2005; Wang et al., 2005). Briefly, slices were placed in an interface chamber (Fine Science Tools) and continuously superfused with oxygenated ACSF (artificial cerebrospinal fluid; 30°C) at 1–3 ml/min. A bipolar stimulating electrode was placed in the stratum radiatum in the CA1 region of the hippocampus to stimulate presynaptic fibres arising from the CA3 pyramidal cells. The fEPSPs (field excitatory post-synaptic potentials) evoked at 0.02 Hz (0.01 ms duration pulses) were recorded in stratum radiatum of the CA1 (dendritic) using low-resistance glass microelectrodes (5–15 MΩ, filled with ACSF). Responses were filtered at 5 kHz and digitized (15–25 kHz) using data acquisition and analysis programs (pClamp9, Axon Instruments). Prior to beginning each experiment, we determined the maximal field potential (fEPSP) amplitude that could be evoked in each slice by gradually increasing the stimulation intensity until the amplitude reached a saturating level. Next, the stimulation intensities that elicited field potentials with 25%, 50% and 75% of maximal amplitude were determined and the half-maximum stimulus strength was selected for recording field potentials every 60 s. Typically, stable baseline measurements were obtained at approx. 30–45 min after placing hippocampal slices in the interface chamber. At this point post-synaptic responses were recorded for at least 10 min prior to the induction of LTP (long-term potentiation). To induce LTP, a tetanizing stimulus of three high-frequency (100 Hz; 1 s duration; 3 min interpulse intervals) pulses was used. Following tetanus, pre-synaptic stimulation was once again delivered every 60 s and the subsequent potentiated post-synaptic responses were recorded for an additional 1 h. In order to determine evoked fEPSP, usually 1 ms of the initial slope of the baseline and post-tetanus responses was measured. Typically the onset of responses was approx. 2–4 ms following a negative DC stimulation. Analysis of the input/output data involved measuring the initial slope of each response following a stimulation of known amplitude ranging from 0–100 μA. For LTP experiments post-tetanic responses were normalized to baseline. For analysis of LTP experiments,

post-tetanic responses were normalized to baseline as is standard in this field. Possible differences in LTP were assessed using a repeated measures ANOVA followed by post-hoc pair-wise comparison with Tukey's *t* test. The α level for all analyses was set at 0.05. In addition, the post-tetanus data was grouped into 10 min bins (10, 20, 30, 40, 50 and 60 min) and pair-wise comparisons made using Tukey's *t* test. Values were considered significantly different if $P<0.05$. PTX (picrotoxin; Sigma–Aldrigh) was measured out and sonicated in 5 ml of ACSF to dissolve into solution. Sonicated PTX was then placed into additional ACSF to reach a final concentration of 100 μM.

Trace- and cued-fear conditioning

Methods were performed as previously described (Chaudhury and Colwell, 2002). The chamber used for training for acquisition of trace-fear conditioning was a 26 cm × 23 cm × 17 cm clear Plexiglass box with a metal grid floor for foot shock delivery (Lafayette Instruments). The chamber for scoring of auditory cued fear was a rectangular box 50 cm × 35.5 cm × 25 cm, constructed of clear plastic. McCormick vanilla extract (~0.5 ml) was painted on to one of the walls of the novel chamber. A computer interfaced to a shock stimulator and speaker delivered the auditory stimulus [CS (conditioned stimulus)] and shock [US (unconditioned stimulus)]. The auditory stimulus (tone) was generated by a speaker producing white noise at 80 dB. The footshock was a 0.5 mA AC current for 2 s. All fear-conditioning procedures were carried out using ABET software (Lafayette Instruments). On the training day, each subject was placed into the conditioning chamber and presented with two CS (white noise)–US (foot shock) pairings. Each pairing was preceded and followed by a 2 min exploration period. For the trace-fear conditioning, the CS–US pairings were comprised of 30 s of white noise (CS), a 2.5 s trace interval, and a 2 s foot shock. For the cued-fear conditioning, the CS–US pairings were comprised of 30 s of white noise (CS) and a 2 s foot shock without the delay. The experimenter observed the mice every 8 s during the 2 min before the first CS–US pairing and the 2 min after the last CS–US pairing for the presence or absence of freezing behaviour (absence of movement). To test short-term fear recall, mice were tested at 2 h post-training. To test longer-term recall, 24 h after training, subjects were individually removed from their home cages (ZT 6 or ZT 18) and taken to a different room for the cued-fear test. This process was repeated daily for 7 days. Each subject was placed in the rectangular box for a total of 8 min. The first 2 min consisted of baseline exploration in the absence of the CS (pre-cue period). During the next 6 min, the CS tone previously used in training was presented (cue period). After the termination of the CS, the subject was allowed to explore the novel context for an additional 60 s (post-cue period). The presence or absence of freezing behaviour was scored every 8 s.
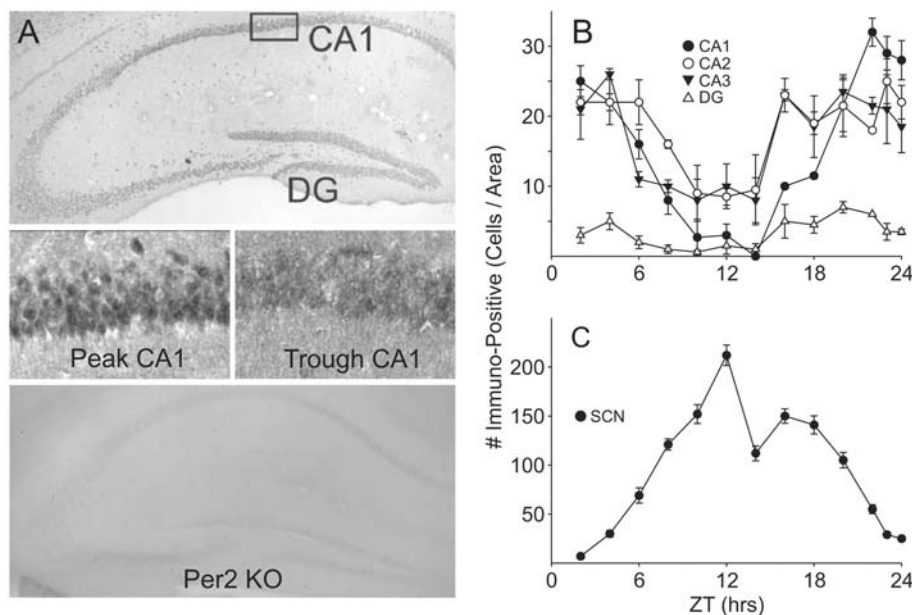
Statistics

Unless otherwise indicated, between-group comparisons were made using ANOVA and post-hoc tests (*t* tests or the Mann–Whitney rank sum tests). In all cases, differences were considered significant if $P<0.05$.

RESULTS

PER2 protein is rhythmically expressed in the hippocampus

To determine whether the pyramidal cell layers within the hippocampus contain parts of the molecular machinery necessary to generate circadian oscillations, we used IHC to examine PER2 protein expression and localization within the various cell layers of the hippocampus. C57 male mice kept under a LD cycle were perfused at different points in the daily cycle (ZT 2, 6, 8, 10, 12, 14, 16, 18, 20, 22, 23 and 24). As is standard in this field, the time of lights-on is defined as ZT 0 and the time of lights-off is defined as ZT 12. IHC was performed in parallel on sections of the hippocampus and SCN

from the same animals. The PER2 immunoreactivity was evident throughout the hippocampus, with expression largely localized to the pyramidal cell body layers of the CA1, CA2, CA3 and DG (Figure 1A). The mean number of immunopositive neurons per hippocampal section varied with the time of day (Figure 1B), with peak counts found between ZT 22 and 4, whereas low counts were measured between ZT 10 and 14. For example, in the CA1 regions, we found 32 ± 2 (mean$\pm$S.E.M., $n=3$) immunopositive cells during the peak of expression and 0 ± 0 cells during the trough ($n=3$; $P=0.001$). Significant differences (Kruskal–Wallis ANOVA, $P<0.01$) were found in CA1, CA2, CA3 and DG, with the latter structure showing the lowest amplitude differences. In the SCN, the rhythms in PER2 immunoreactivity was robust, as expected (Figure 1C). Our IHC protocol did not detect any positive staining in tissue from a *Per2*-null mutant mouse (Figure 1A). Other control experiments in which the primary antibody was not added or the primary antibody was pre-absorbed with a PER2 peptide did not exhibit any positive staining (Supplementary Figure S1 at http://www.asnneuro.org/an/001/an001e012add.htm). Analysis with confocal microscopy indicates that the PER2 immunoreactivity is found in the nucleus as well as the cytoplasm of hippocampal cells (Supplementary Figure S2 at http://www.asnneuro.org/an/001/an001e012add.htm).
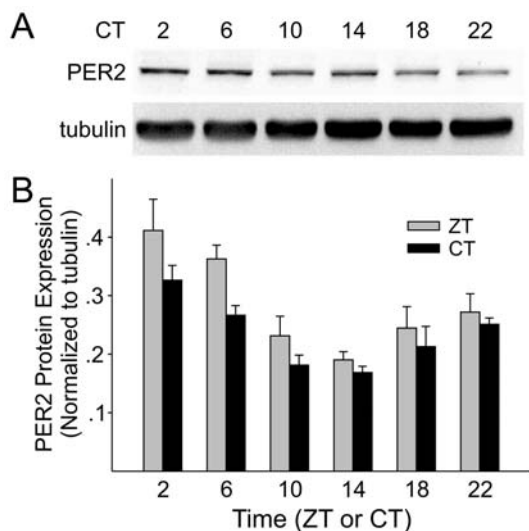

Figure 1   PER2 is rhythmically expressed in the mouse hippocampus
Mice were held in an LD cycle and brains collected at different times in the daily cycle (ZT 2, 4, 6, 8, 10, 12, 14, 16, 18, 20, 22 and 24). Sections of the brains containing the hippocampus and SCN were stained for PER2 expression using IHC. (**A**) IHC expression was largely localized to the hippocampal regions known as CA1, CA2, CA3 and DG. The patterns of staining varied as a function of time of day, and examples of immunoreactivity in the peak (ZT 2) and trough (ZT 14) of the daily rhythm are shown. The weak, poorly localized staining at ZT 14 is likely to still represent positive immunolabelling. Keeping the IHC conditions constant, there was no positive immunoreactivity in the hippocampus of a *Per2*-null mutant. Similarly pre-absorption controls lacked this diffuse immunolabelling (Supplementary Figure S1 at http://www.asnneuro.org/an/001/an001e012add.htm). KO, knockout. (**B**) The number of PER2 immunopositive neurons were counted by observers blinded to the experimental conditions. Levels of PER2 expression in the hippocampus varied as a function of time of day, with peak expression in the late night/early morning and troughs of expression in the late day/early night. (**C**) In contrast, peak PER2 expression in the SCN was out-of-phase with the hippocampus, with highest expression at the late day/early night. At each time point $n=4$. Values are means$\pm$S.E.M.

In order to provide a more quantitative analysis of PER2 expression, we measured protein levels from the hippocampus of mice sampled throughout the daily cycle (ZT 2, 6, 10, 14, 18 or 22) using Western blot analysis (Figure 2). Total PER2 protein expression was normalized to tubulin which does not vary as a function of time of day (see the Materials and methods section). The PER2 protein bands were not detected in controls in which the PER2 primary antibody was pre-absorbed or omitted (results not shown). Consistent with our IHC results, the PER2 expression varied significantly as a function of time of day (ANOVA, $P=0.007$; Figure 2B) with peak expression at ZT 2 and the lowest expression at ZT 14. For example, absorbance measurements of PER2 (normalized to loading controls) at the peak of expression was 0.41 ± 0.05 and 0.19 ± 0.01 at the trough ($n=3$; $P=0.01$). This daily rhythm in PER2 expression persisted in animals held in DD. Under these conditions, activity levels were monitored with running wheels, and activity onset was defined as CT 12. Hippocampal tissue obtained throughout the daily cycle (CT 2, 6, 10, 14, 18 or 22) also exhibited significant circadian differences in PER2 expression (ANOVA, $P=0.01$; Figure 2B). For example, absorbance measurements of PER2 (normalized to loading controls) at the peak of expression was 0.33 ± 0.02 compared with 0.17 ± 0.01 at the trough ($n=6$; $P=0.01$).

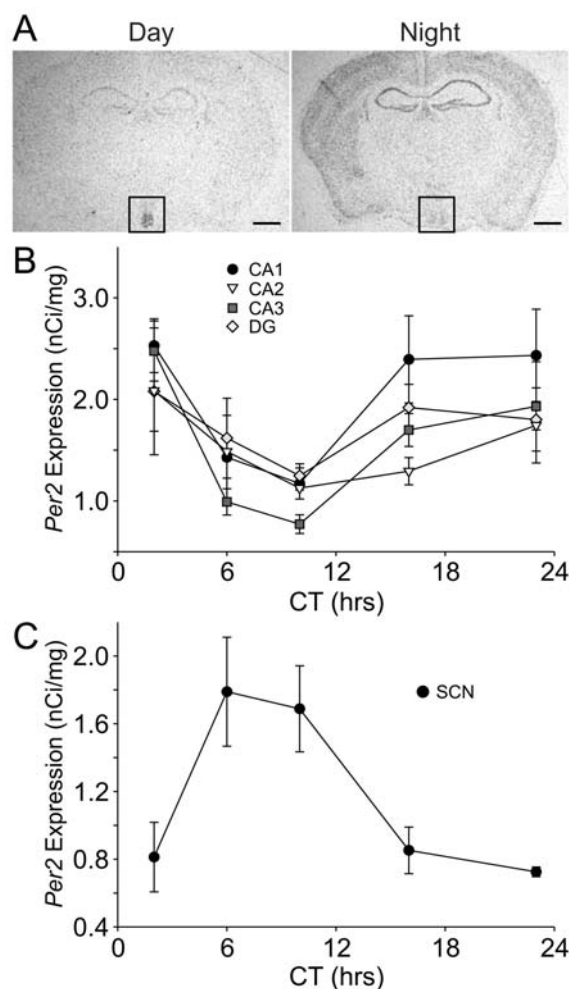### *Per2* mRNA is rhythmically expressed in the hippocampus

In order to examine whether the mRNA coding for *Per2* is rhythmic in the hippocampus (Wakamatsu et al., 2001), we

used ISH to measure *Per2* mRNA in the hippocampus and SCN of mice throughout the daily cycle (CT 2, 6, 10, 16 and 23). Activity levels were monitored with running wheels, and activity onset was defined as CT 12. ISH was performed in parallel on tissue from the hippocampus and SCN (Figure 3A). Expression of *Per2* mRNA was observed throughout the rostrocaudal extent of the hippocampus and was largely restricted to the pyramidal cell layers and the DG. For each of the cell populations, the level of *Per2* expression varied with the circadian cycle with peak expression between CT 23 and 2, whereas the troughs were at CT 10 (Figure 3B). Analysis of the absorbance measurements of *Per2* expression (normalized

Figure 3 A diurnal rhythm in *Per2* mRNA in the hippocampus as measured by ISH
Mice were held in DD and wheel-running activity was measured to determine circadian phase. ISH was used to measure *Per2* expression in the hippocampus and SCN ($n=3$–4 per group). (**A**) Film images of ISH for *Per2* on tissue sections taken from mice sacrificed during the peak and trough of expression. Scale bar=1 mm. (**B**) Levels of *Per2* expression in the hippocampus varied as a function of time of day, with the strongest hybridization signal in the late night/early morning. (**C**) Peak *Per2* expression in the SCN was out-of-phase with the hippocampus, with the strongest hybridization signal at mid-day. At each time point $n=3$–4. Values are means ± S.E.M.

Figure 2 Western blot analysis indicates that hippocampal PER2 expression exhibits a circadian rhythm
Mice were held in DD and wheel-running activity was measured to determine circadian phase. (**A**) Example of Western blots measuring PER2 expression in whole hippocampal tissue as a function of time of day. Tubulin protein expression was measured as a control for loading and did not vary as a function of time of day (see the Materials and methods section). (**B**) Levels of PER2 protein expression (normalized to tubulin) varied as a function of time of day in both LD and DD conditions.
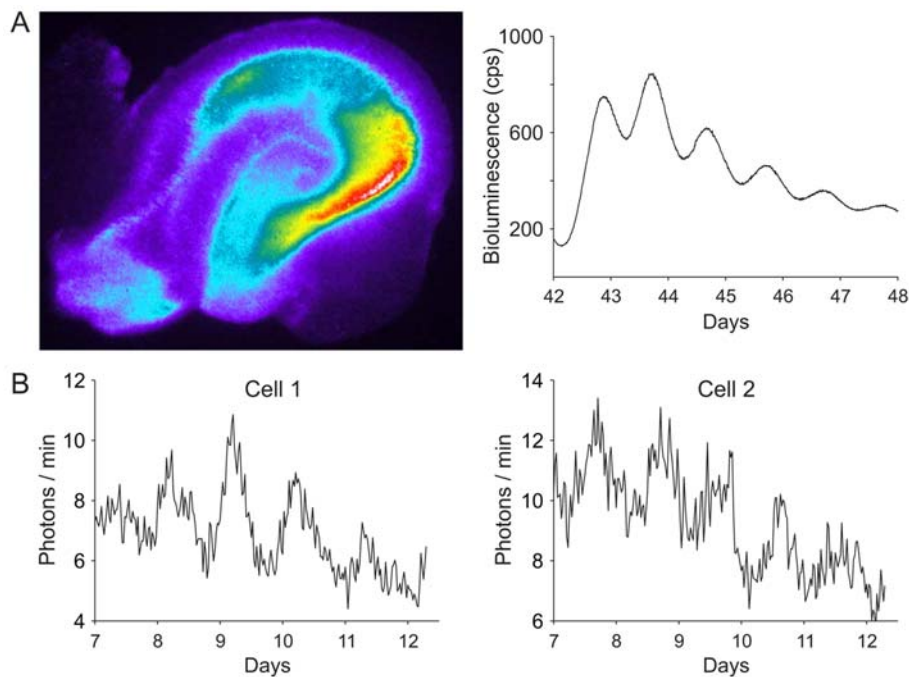
to background) indicated that the levels of expression were significantly different (as measured using ANOVA) in the CA1 ($P<0.02$), CA3 ($P<0.001$) and DG ($P<0.03$) regions. For example, in the CA1 cell layer, the absorbance measurements at the peak of expression was 0.25 ± 0.03, whereas *Per2* expression decreased to 0.12 ± 0.01 at the trough ($n=3$; $P=0.01$). For comparison, in the SCN (Figure 3C), the mean absorbance of *Per2* was higher at subjective day (CT 6, 5.27 ± 0.82 absorbance units; $n=7$) than in the subjective night (CT 16, 2.15 ± 0.37 absorbance units; $n=7$, $P<0.01$). The *Per2* sense probe did not exhibit labelling in the brain under identical hybridization conditions (results not shown).

Rhythms in *Per2*::LUC expression in the isolated hippocampus

To determine whether circadian rhythms of *Per2* expression in the hippocampus are autonomous, we used an optical reporter that allowed us to follow expression from isolated hippocampal slices maintained in organotypic culture (Figure 4A). These slice cultures were prepared from knockin mice in which the endogenous *Per2* gene is replaced by a fusion of *Per2* and the firefly luciferase gene (*luc*+), such that an *Per2*::LUC fusion protein is expressed, reflecting both transcriptional and post-transcriptional regulation of the *Per2* locus (Yoo et al., 2004). Hippocampal slices produced

clear circadian rhythms of PER2::LUC bioluminescence when monitored in the luminometer ($n=4$; period$=25.08\pm0.13$ h; Figure 4A). These rhythms peaked at ~ZT 20, i.e. ~4 h before light onset in the LD cycle to which the mice had been entrained. This is somewhat earlier than indicated by Western blot analysis, consistent with the short effective half-life of PER2::LUC bioluminescence resulting from substrate inhibition of the luciferase enzyme. The rhythms gradually declined in amplitude over several days in culture, but amplitude could be restored by a medium change (results not shown), as reported previously for other brain regions (Abe et al., 2002). Cerebellar slices, although producing similar mean levels of PER2::LUC bioluminescence, were non-rhythmic ($n=4$; results not shown). Thus hippocampal rhythms of *Per2* expression are produced without input from the SCN or other brain regions, but may require such input for persistence and synchronization (Whitmore et al., 1998; Yamazaki et al., 2000; Liu et al., 2007).

To determine the location of rhythmic *Per2* expression within the hippocampus, we performed bioluminescence imaging of a hippocampal slice cultured from a *Per2*::LUC mouse. Average levels of *Per2*::LUC bioluminescence [in A/D (analogue-to-digital) units per pixel, with background subtracted] were 89.1 in the DG, 92.8 in CA3, 67.2 in CA1 and 54.5 in the cingulate cortex. Damped circadian rhythmicity was evident in the CA1, CA3 and DG regions,

Figure 4   Circadian rhythm of PER2::LUC bioluminescence in isolated hippocampus
(**A**) Organotypical hippocampal slices obtained from PER2::LUC transgenic mice were maintained in culture, and bioluminescence was recorded by imaging (left-hand panel; bioluminescence intensity on a pseudocolour scale) or luminometry (right-hand panel). Rhythmicity of bioluminescence damped over a period of several days. The media was changed immediately before these luminescence measurements began. (**B**) Recordings of PER2::LUC rhythms from individual cells over a 5-day period. The *x*-axis label refers to the days in culture.
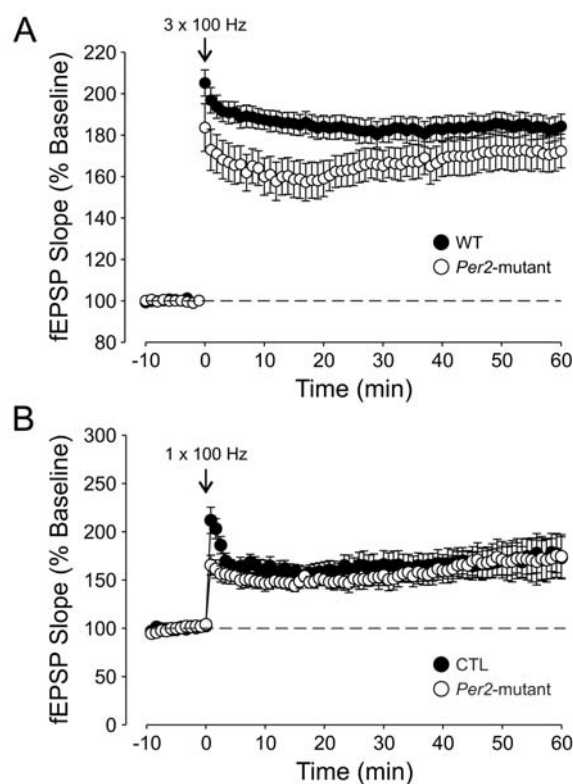
and was rather prominent in the cingulate cortex. We were able to discriminate a few single cells near the border of CA1 and CA3, and observed circadian rhythms of different phases (Figure 4B). These results raise the possibility that autonomous circadian clocks operate within the hippocampus.

Per2-mutant mice exhibit deficits in hippocampal LTP

To determine whether *Per2* may play a role in regulating synaptic physiology, we examined LTP in *Per2*-mutant mice (see Supplementary Figure S3 at http://www.asnneuro.org/an/001/an001e012add.htm). Since PER2 is a transcriptional regulator, we first sought to determine the effect of mutations in this gene on strong LTP. This type of synaptic plasticity is long-lasting and has been shown to be dependent upon protein synthesis (Impey et al., 1996; Bekinschtein et al., 2007). For these experiments, we stimulated the SC (Schaffer collaterals) and measured the evoked fEPSPs in the CA1 dendritic region of hippocampal slices prepared from WT and *Per2*-mutant mice. After establishing a stable baseline, LTP was induced by the delivery of three bursts of high-frequency stimulation (3×100 Hz; 1 s duration; 3 min interstimulus intervals), after which evoked responses were recorded for 60 min. These experiments were carried out in the presence of 100 µM PTX (continuous bath application) to remove any contribution from GABA$_A$ receptors. Using the strong tetanizing protocol, the fEPSP slope of WT mice was increased to $192 \pm 8\%$, $185 \pm 8\%$ and $184 \pm 8\%$ of baseline at 10 min, 30 min and 60 min after tetanus ($n=6$). In contrast, the LTP traces from *Per2*-mutant animals showed a reduced magnitude of LTP (Figure 5A). The *Per2*-mutant mice exhibited an average fEPSP slope of $170 \pm 12\%$, $159 \pm 10\%$ and $171 \pm 12\%$ of baseline at 10 min, 30 min and 60 min after tetanus ($n=8$). The magnitude of the fEPSP slopes was significantly smaller than for WT when measured at 10, 20, 30 and 40 min after tetanus ($P<0.05$). We also examined the impact of the loss of *Per2* on the magnitude of the LTP evoked by a weaker stimulus (1×100 Hz, 1 s duration; Figure 5B). This weak protocol produces a synaptic potentiation that is shorter and not dependent upon protein synthesis (Frey et al., 1993). There was no significant difference between LTP recorded from WT and *Per2*-mutant animals [WT, $166 \pm 13\%$ ($n=7$); *Per2*-mutant, $158 \pm 12\%$ ($n=7$); $P>0.05$]. Thus the impact of a mutation in *Per2* was selective for the synaptic potentiation evoked by the strong LTP protocol.

Previous work indicates that *Per2* may be involved in regulating the amount of vesicular glutamate transporter 1 (Yelamanchili et al., 2006) and could alter LTP indirectly through an inhibition of excitatory synaptic transmission within the hippocampus. To test this possibility, we carried out experiments designed to determine whether there was a difference in baseline-evoked fEPSP in hippocampal slices prepared from WT or *Per2*-mutant mice. For these experiments, we varied the stimulus intensity and recorded the resulting slope to characterize the IO (input/output) relationship for these evoked responses. A change in the gain of

Figure 5 *Per2*-mutant mice exhibit abnormal LTP in the hippocampus
(**A**) LTP measured by stimulating the SC and recording the fEPSP from the CA1 dendritic layer in brain slices from WT (●) and *Per2*-mutant (○) mice. Data are presented as the fEPSP slope (normalized as a percentage of the baseline). The high-frequency stimulation (3×100 Hz; 1 s duration; 3 min interstimulus intervals) was given at time$=0$. Experiments were carried out in the presence of the GABA$_A$ blocker PTX. (**B**) In contrast, the magnitude of LTP evoked by a weaker stimulation (1×100 Hz) did not significantly vary between WT (●) and *Per2*-mutant (○) mice.

IO curve would indicate a change in sensitivity of the neuron to the excitatory input. No differences were found in the IO curves measured for the fEPSP of the two genotypes (Table 1). Other electrophysiological parameters of the evoked responses were found not to vary significantly between the WT and mutant mice (Table 1). These data rule out any gross changes in basic excitatory synaptic transmission or excitability of the mutant hippocampal brain slices.

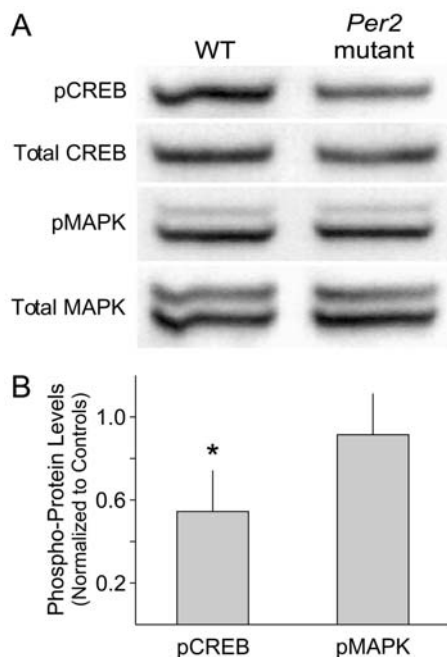## *Per2*-mutant mice exhibit deficits in p-CREB protein expression

Our physiological analysis found that a mutation in *Per2* selectively altered the magnitude of LTP evoked by a strong stimulation protocol. Previous work has shown that the phosphorylation of CREB is a critical step in the signalling pathway leading to strong LTP and certain long-term memories (Lonze and Ginty, 2002; Bozon et al., 2003). We carried out Western blot analysis with an antibody that recognizes CREB phosphorylation at Ser[133] (p-CREB) to determine whether a mutation in *Per2* impacts the activated

Table 1 Per2-mutant mice do not exhibit deficits in basic synaptic transmission
Values are means ± S.E.M.

Measurement	WT	Per2 mutant
fEPSP slope (mV/ms)	−0.74 ± 0.07	−0.92 ± 0.12
Peak amplitude (mV)	−1.39 ± 0.21	−1.67 ± 0.17
Duration (ms)	30.93 ± 0.67	30.69 ± 0.55
IO slope		
10 mV	−0.05 ± 0.02	−0.06 ± 0.02
15 mV	−0.54 ± 0.08	−0.51 ± 0.06
20 mV	−1.06 ± 0.13	−0.94 ± 0.08
25 mV	−1.32 ± 0.17	−1.28 ± 0.09

state of this signalling cascade (Figure 6). To control for potential variations in loading, the absorbance units of bands for each protein of interest were first normalized to the absorbance values obtained for tubulin loading control bands in each lane. Normalized absorbance values were then expressed as a percentage of the levels seen in WT samples or as a ratio of phosphorylated protein/total protein. We found that the ratio of p-CREB/total CREB expression was significantly decreased in the mutant mice under baseline conditions [WT, 1.7 ± 0.06 ($n=3$); mutant, 0.9 ± 0.1 ($n=3$); $P<0.05$]. This effect was selective for the CREB pathway in that the ratio of phosphorylated to total ERK (p-ERK/total ERK) in mutant mice was comparable with controls [WT, 0.55 ± 0.05 ($n=3$); mutant, 0.50 ± 0.04 ($n=3$); $P>0.05$]. The
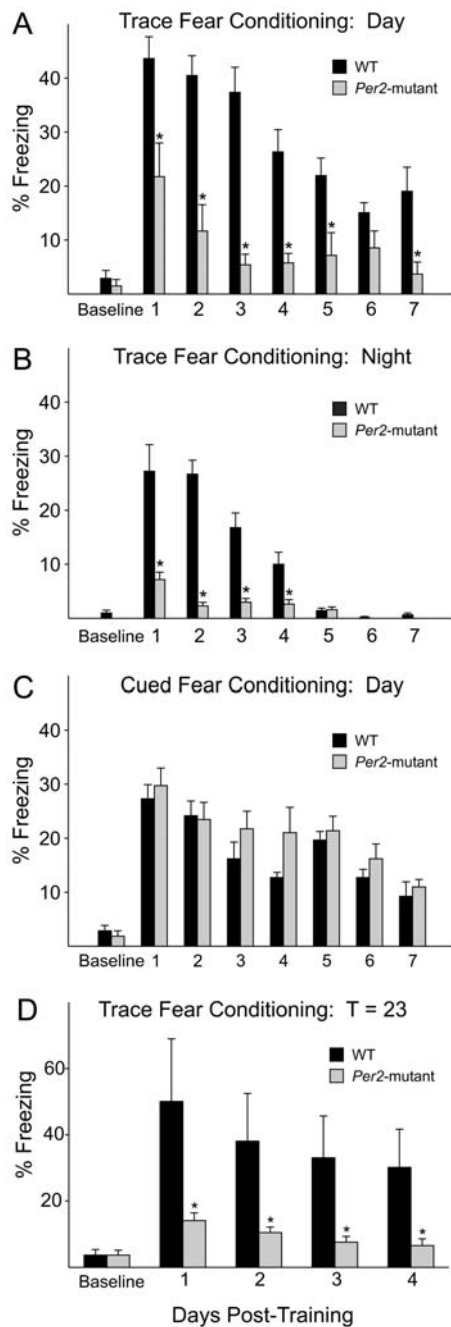

Figure 6 p-CREB is down-regulated in Per2-mutant mice
(**A**) Western blot showing hippocampal p-CREB, total CREB, p-ERK (pMAPK) and total ERK (total MAPK) protein expression in WT and Per2-mutant mice (normalized to tubulin). (**B**) p-CREB and p-ERK protein expression was normalized to total CREB and total ERK expression respectively. These p-CREB/total CREB and p-ERK/total ERK measurements from Per2-mutant mice were compared with data from WT mice. Values are means ± S.E.M., *$P<0.05$.

decrease in CREB phosphorylation was also regionally selective as there were no significant changes in the p-CREB/total CREB ratio in SCN tissue [WT, 0.88 ± 0.07 ($n=3$); mutant, 0.99 ± 0.06 ($n=3$)]. Similarly, there were no significant changes in the p-CREB/total CREB ratio in the whole brain excluding the hippocampus [WT, 0.84 ± 0.13 ($n=3$); mutant, 1.0 ± 0.15 ($n=3$)]. Thus p-CREB levels are selectively reduced in the hippocampus of Per2-mutant mice.

Per2-mutant mice exhibit deficits in the recall of trace-fear conditioning

To determine whether Per2 has a functional role in learning and memory, we tested Per2-mutant mice for deficits in the acquisition and recall of trace-fear conditioning. Mice were trained during the day (ZT 6) or night (ZT 18) to associate an initially neutral tone (CS) to a biologically relevant event, a foot shock (US). A brief temporal interval or 'trace' of 2.5 s was placed between the tone (80 dB; 2.8 kHz) and the onset of the foot shock (0.5 mA; 2 s). This trace increases the hippocampal-dependence of the behavioural response (McEchron et al., 1998; Quinn et al., 2002). In this assay, fear was measured as inactivity or 'freezing' after the stimulus. Freezing is a typical defensive response displayed by rodents following exposure to aversive stimuli. Once the association between the CS and US was acquired, Per2-mutant and C57 mice were tested once a day (ZT 6 or 18) for recall, for a total of 7 days.

We found that Per2-mutant mice did not show deficits in their ability to acquire trace-fear learning. For example, freezing after the last CS–US pairing was $52 \pm 6\%$ ($n=8$) in the mutant mice compared with $50 \pm 7\%$ ($n=8$) in WT controls. In addition, the short-term ability of the Per2-mutant mice to recall the trace-fear conditioning at 2 h post-training was not significantly different from WT controls. At 2 h post-training, Per2-mutant mice showed $8.8 \pm 2\%$ freezing behaviour compared with $9.6 \pm 2\%$ freezing in controls ($P>0.05$; results not shown). However, the ability of the Per2-mutant mice to recall the fear conditioning at 24 h to 7 days post-training was severely compromised (Figure 7A). In Per2-mutant mice trained and tested for recall during the day (ZT 6), recall of fear conditioning was significantly decreased by the first day of testing, with $22 \pm 6\%$ freezing behaviour compared with $44 \pm 4\%$ freezing in WT animals ($n=8$; $P<0.05$). By day 7 post-training, mutant mice exhibited freezing behaviour $4 \pm 2\%$ of the time, whereas WT mice exhibited freezing behaviour $20 \pm 5\%$ of the time ($n=6$; $P<0.05$). We also examined the recall of fear conditioning in mice trained and tested during the night (ZT 18). Again, the Per2-mutant mice exhibited significantly lower recall than WT controls (Figure 7B; $P<0.01$). For both genotypes, the recall during the night was significantly lower than recall during the day (Chaudhury and Colwell, 2002; Eckel-Mahan et al., 2008). Finally, we examined the performance of Per2-mutant mice on cued-fear conditioning (Zueger et al., 2006). We found that Per2-mutant mice did not show deficits in their ability to acquire or recall cue-fear learning (Figure 7C). Therefore the

Figure 7 *Per2*–mutant mice exhibit severe deficits in the recall of trace–fear conditioning

(**A**) Levels of trace-fear conditioning recall in *Per2*-mutant mice tested at 24 h intervals post-training during the day (ZT 6) show severe deficits in their ability to recall learning. (**B**) This deficit in trace-fear recall persisted in *Per2*-mutant mice trained and tested during the night (ZT 18). Fear-learning behaviour was measured as the percentage freezing over the total testing time. (**C**) In contrast, the *Per2*-mutant mice did not exhibit deficits in recall of cued-fear conditioning. (**D**) The *Per2*-mutant mice exhibit deficits in the recall of trace-fear conditioning when held on a 23-h cycle. Values are means ± S.E.M., *$P<0.05$.

recall deficits exhibited by the *Per2*-mutant mice are selective for the trace-fear conditioning.

The *Per2*-mutant mice exhibit a shorter circadian period (Zheng et al., 1999) than WT mice, and a recent study suggests that altering the period length to which subjects are entrained can impact learning in humans (Wright et al., 2006). This raises the possibility that the shorter endogenous period of the mutant mice could contribute to the deficits in recall, because of a greater mismatch with the 24 h period of the LD cycle. We examined this possibility by holding both WT and *Per2*-mutant mice in a 23 h LD cycle (11.5 h/11.5 h), which more closely approximates the endogenous free-running period of the mutant mice. We found that *Per2*-mutant mice did not show deficits in their ability to acquire trace-fear learning. For example, freezing after the last CS–US pairing was 24 ± 7% (*n*=8) in the mutant mice compared with 25 ± 3% (*n*=8) in WT controls. However, the recall of the *Per2*-mutant mice was still significantly lower than controls (Figure 7D). Overall, our results demonstrate that the *Per2*-mutant mice exhibited deficits in the recall, but not the acquisition, of trace-fear conditioning.

DISCUSSION

The results of the present study demonstrate that the principal pyramidal neurons of the hippocampal complex express *Per2* mRNA and protein. This expression is rhythmic, and the time of peak expression is out-of-phase with that in the SCN. With these data, the hippocampus joins a growing list of brain regions in which rhythms of *Per* expression have been described. This group includes other brain regions involved in behavioural plasticity, including the amygdala and the DG (Lamont et al., 2005). This extra-SCN expression raises the possibility that a variety of brain regions may be able to generate circadian oscillations. It is also possible that so-called 'clock genes' such as *Per2* may play functional roles as transcriptional regulators independent of circadian function. In this regard, the finding that *Per2* expression is rhythmic when the hippocampus is isolated from the SCN in culture is an important observation. This finding demonstrates that the hippocampus is indeed capable of generating independent circadian oscillations. Our results raise the possibility that cell-autonomous circadian clocks operate in several sub-regions within the hippocampus, but that cells desynchronize in the absence of the SCN (Welsh et al., 2004). In mammals, neurons in the hippocampus (the present study), olfactory bulb (Abraham et al., 2005), SCN (Yoo et al., 2004) and other brain regions (Abe et al., 2002) have now been shown to generate independent oscillations in circadian gene expression.

In the present study, we carefully describe the phase relationship between *Per2* expression in the hippocampus and SCN. We found them to be in anti-phase with each other, i.e.

when expression of Per2 mRNA and protein peaked in the hippocampus, these levels were near their trough in the SCN. Future studies will need to determine how these phase relationships are altered in response to environmental perturbations and disease. The hippocampus is one of the brain regions strongly implicated in the pathophysiology of mood disorders (Drevets et al., 2008). The 'social zeitgeber theory' of depression postulates that life stresses can produce a misalignment of the phase relationship between the central clock and the environment and that this misalignment could have a negative impact on nervous system function and health (Ehlers et al., 1988; Grandin et al., 2006; McClung, 2007). The results of the present study highlight the importance of coupling between circadian oscillators within the nervous system. The fact that both the hippocampus and the SCN have distinct clockwork mechanisms raise the possibility that desynchronization between cell populations within the nervous system may contribute to mood disorders.

This pool of data contributes to the view that the circadian system is comprised of multiple oscillatory components, with the role of the SCN being a master timer synchronizing these disparate cell populations (Stratmann and Schibler, 2006; Liu et al., 2007). With this new view of clock genes and circadian organization, it becomes critical to determine the tissue-specific function of these genes. Logically, local rhythms in clock gene expression could serve to control the temporal programme of gene expression and physiology specific to the hippocampus, as recently demonstrated in the liver (Kornmann et al., 2007). However, unfortunately, we still do not know much about the functional significance of clock gene expression outside of the SCN.

We first examined the function of the clock gene Per2 in the hippocampus using a physiological analysis. Synapses within the hippocampus undergo history-dependent changes in the strength of synaptic transmission. This synaptic plasticity is widely studied as a possible cellular mechanism of behavioural plasticity including learning and memory (Morris et al., 1990). While recognizing that there are advantages to conditional- or regional-specific mutations; as a first step, we examined LTP in a line of mice containing a mutation that renders the PER2 protein non-functional (Zheng et al., 1999). We found that Per2-mutants exhibit reduced magnitude of LTP as measured at the SC/CA1 synaptic connection. Basic excitatory synaptic transmission at the SC/CA1 synapse was not altered in the mutant mice. We found that the Per2-mutant mice exhibited altered levels of p-CREB, but not p-ERK. The levels of total CREB were not impacted by deficiencies in Per2; only the activated state of this signalling pathway was affected, as measured by phosphorylation. This biochemical consequence of a mutation in Per2 was regionally specific, as the deficit was not seen in SCN tissue. There is abundant evidence that CREB or CREB-binding proteins play a role in some forms of LTP and long-term memory (e.g. Lonze and Ginty, 2002; Bozon et al., 2003; Wood et al., 2006). Our results raise the possibility that Per2-related deficits in intracellular signalling pathways may be an

important part of the observed deficits in LTP. Interestingly, recent work indicates that the levels of cAMP and MAPK (mitogen-activated protein kinase) activity in the hippocampus exhibit circadian oscillations (Eckel-Mahan et al., 2008). Previous work in Aplysia implicates the circadian gating of the MAPK pathway as the mechanistic control point for circadian regulation of sensitization (Lyons et al., 2006). Regardless of the mechanism, these are the first results suggesting a link between the expression of clock genes and LTP. This link will need to be further pursued with other types of transgenic models and experimental approaches.

Given the deficits that we observed in synaptic plasticity and CREB phosphorylation, we wanted to test the performance of the Per2-mutant mice on learned behavioural tasks. Trace-fear conditioning is a simple, easy to learn task with well-defined circuitry that includes the hippocampus (Maren and Quirk, 2004; Fanselow and Poulos, 2005). We found that the Per2-mutant mice exhibited profound deficits in the longer-term recall, but not in the acquisition or short-term recall, of trace-fear conditioning. The Per2-mutant mice did not alter performance in the acquisition or recall of cued-fear conditioning (Zueger et al., 2006). Previous work suggests that trace-fear conditioning requires an intact medial pre-frontal cortex and hippocampus, whereas cued-fear conditioning does not (Kim and Fanselow, 1992; Ji et al., 2003; Maren and Quirk, 2004; Runyan et al., 2004; Fanselow and Poulos, 2005). The difference in the impact of the loss of functional PER2 on trace- compared with cued-fear conditioning is at least consistent with the possibility that the dysfunction in hippocampal physiology and intracellular signalling described above may underlie the deficits in recall. However, PER2 is a transcriptional regulator that is expressed in a number of brain regions and the present results do not allow us to specify the anatomical site responsible for the impact of the loss of Per2 on trace-fear conditioning. Our behavioural results do provide a clear demonstration that a mutation in a circadian-related gene selectively influences the recall of some, but not all, forms of learned behaviour.

The deficits in the recall of trace-fear conditioning were still observed when mice were placed on a short T-cycle to control for the impact of the shorter period of the mutant mice. In previous work, humans placed on a 24.6 T-cycle who were unable to synchronize to this LD cycle exhibited deficits in a variety of learning and vigilance tasks (Wright et al., 2006). The experimental design of the present study did not directly seek to determine whether poorly synchronized mice also show deficits in performance. However, it is worth noting that the freezing after training for both WT and Per2-mutants was notably lower when the mice were held on the T=23 LD cycle. Future studies will need to specifically test the hypothesis that proper alignment between the LD cycle and the circadian system impacts learning and memory tasks.

Our findings complement earlier work reporting that mPer1-deficient mice exhibit deficits in place preference conditioning (Abarca et al., 2002), whereas Clock-mutant

mice exhibit a stronger preference for cocaine (McClung et al., 2005). Also, deficits in cued- and contextual-fear conditioning have been described in NPAS2 (neuronal PAS domain protein 2)-deficient mice (Garcia et al., 2000). In *Drosophila*, *Per*-null mutations disrupted long-term memory for courtship behaviour (Sakai et al., 2004). These deficits were rescued by the induction of a *Per* transgene, whereas the overexpression of *Per* enhanced long-term memory formation. The loss of other circadian genes (*Clock*, *Timeless* and *Cycle*) did not influence learned behaviour in flies, suggesting a special role for the *Per* gene. Taken together, these results establish a link between genes involved in the generation of circadian oscillations and the recall of learned behaviour. We suggest that the rhythmic expression of clock genes in brain regions outside of the SCN may be part of the mechanism by which the circadian system imposes a temporal order on cognitive functions in mammals.

REFERENCES

Abarca C, Albrecht U, Spanagel R (2002) Cocaine sensitization and reward are under the influence of circadian genes and rhythm. Proc Natl Acad Sci USA 99:9026–9030.

Abe M, Herzog ED, Yamazaki S, Straume M, Tei H, Sakaki Y, Menaker M, Block GD (2002) Circadian rhythms in isolated brain regions. J. Neurosci 22:350–356.

Abraham U, Prior JL, Granados-Fuentes D, Piwnica-Worms DR, Herzog ED (2005) Independent circadian oscillations of Period1 in specific brain areas *in vivo* and *in vitro*. J Neurosci 25:8620–8626.

Bae K, Jin X, Maywood ES, Hastings MH, Reppert SM, Weaver DR (2001) Differential functions of mPer1, mPer2, and mPer3 in the SCN circadian clock. Neuron 30:525–536.

Bekinschtein P, Cammarota M, Igaz LM, Bevilaqua LR, Izquierdo I, Medina JH (2007) Persistence of long-term memory storage requires a late protein synthesis- and BDNF-dependent phase in the hippocampus. Neuron 53:261–277.

Bozon B, Kelly A, Josselyn SA, Silva AJ, Davis S, Laroche S (2003) MAPK, CREB and zif268 are all required for the consolidation of recognition memory. Philos Trans R Soc Lond B Biol Sci 358:805–814.

Chaudhury D, Colwell CS (2002) Circadian modulation of learning and memory in fear-conditioned mice. Behav Brain Res 133:95–108.

Chaudhury D, Wang LM, Colwell CS (2005) Circadian regulation of hippocampal long-term potentiation. J Biol Rhythms 20:225–236.

Chaudhury D, Loh DH, Dragich JM, Hagopian A, Colwell CS (2008) Select cognitive deficits in vasoactive intestinal peptide deficient mice. BMC Neurosci 9:63.

Dijk DJ, Duffy JF, Czeisler CA (1992) Circadian and sleep/wake dependent aspects of subjective alertness and cognitive performance. J Sleep Res 1:112–117.

Drevets WC, Price JL, Furey ML (2008) Brain structural and functional abnormalities in mood disorders: implications for neurocircuitry models of depression. Brain Struct Funct 213:93–118.

Eckel-Mahan KL, Phan T, Han S, Wang H, Chan GC, Scheiner ZS, Storm DR (2008) Circadian oscillation of hippocampal MAPK activity and cAMP: implications for memory persistence. Nat Neurosci 119:1074–1082.

Ehlers CL, Frank E, Kupfer DJ (1988) Social zeitgebers and biological rhythms. Arch Gen Psychiatry 45:948–952.

Ellenbogen JM, Payne JD, Stickgold R (2006) The role of sleep in declarative memory consolidation: passive, permissive, active or none? Curr Opin Neurobiology 16:716–722.

Fanselow MS, Poulos AM (2005) The neuroscience of mammalian associative learning. Annu Rev Psychol 56:207–234.

Fernandez RI, Lyons LC, Levenson, J, Khabour O, Eskin A (2003) Circadian modulation of long-term sensitization in *Aplysia*. Proc Natl Acad Sci USA 100:14415–14420.

Frey U, Huang YY, Kandel ER (1993) Effects of cAMP simulate a late stage of LTP in hippocampal CA1 neurons. Science 260:1661–1664.

Garcia JA, Zhang D, Estill SJ, Michnoff C, Rutter J, Reick M, Scott K, Diaz-Arrastia R, McKnight SL (2000) Impaired cued and contextual memory in NPAS2-deficient mice. Science 88:2226–2230.

Gau D, Lemberger T, von Gall C, Kretz O, Minh N, Gass P, Schmid W, Schibler U, Korf HW, Schutz G (2002) Phosphorylation of CREB Ser142 regulates light-induced phase shifts of the circadian clock. Neuron 34:245–253.

Grandin LD, Alloy LB, Abramson LY (2006) The social zeitgeber theory, circadian rhythms, and mood disorders: review and evaluation. Clin Psychol Rev 26:679–694.

Hampp G, Ripperger JA, Houben T, Schmutz I, Blex C, Perreau-Lenz S, Brunk I, Spanagel R, Ahnert-Hilger G, Meijer JH, Albrecht U (2008) Regulation of monoamine oxidase A by circadian-clock components implies clock influence on mood. Curr Biol. 18:678–683.

Impey S, Mark M, Villacres EC, Poser S, Chavkin C, Storm DR (1996) Induction of CRE-mediated gene expression by stimuli that generate long-lasting LTP in area CA1 of the hippocampus. Neuron 16: 973–982.

Ji JZ, Wang XM, Li BM (2003) Deficit in long-term contextual fear memory induced by blockade of β-adrenoceptors in hippocampal CA1 region. Eur J Neurosci 17:1947–1952.

Kandel ER (2001) The molecular biology of memory storage: a dialogue between genes and synapses. Science 294:1030–1038.

Kim JJ, Fanselow MS (1992) Modality-specific retrograde amnesia of fear. Science 256:675–677.

Ko CH, Takahashi JS (2006) Molecular components of the mammalian circadian clock. Human Mol Genet 2:R271–R277.

Kornmann B, Schaad O, Bujard H, Takahashi JS, Schibler U (2007) System-driven and oscillator-dependent circadian transcription in mice with a conditionally active liver clock. PLoS Biol 5:e34.

Lambert CM, Machida KK, Smale L, Nunez AA, Weaver DR (2005) Analysis of the prokineticin 2 system in a diurnal rodent, the unstriped Nile grass rat (*Arvicanthis niloticus*). J Biol Rhythms 20:206–218.

Lamont EW, Robinson B, Stewart J, Amir S (2005) The central and basolateral nuclei of the amygdala exhibit opposite diurnal rhythms of expression of the clock protein Period2. Proc Natl Acad Sci USA 102: 4180–4184.

Liu AC, Lewis WG, Kay SA (2007) Mammalian circadian signaling networks and therapeutic targets. Nat Chem Biol 3:630–639.

Lonze BE, Ginty DD (2002) Function and regulation of CREB family transcription factors in the nervous system. Neuron 35:605–623.

Lyons LC, Collado MS, Khabour O, Green CL, Eskin A (2006) The circadian clock modulates core steps in long-term memory formation in *Aplysia*. J Neurosci 26:8662–8671.

Maren S, Quirk GJ (2004) Neuronal signaling of fear memory. Nat Rev Neurosci 5:844–852.

McClung CA (2007) Circadian genes, rhythms and the biology of mood disorders. Pharmacol Therapeutics 114:222–232.

McClung CA, Sidiropoulou K, Vitaterna M, Takahashi JS, White FJ, Cooper DC, Nestler EJ (2005) Regulation of dopaminergic transmission and cocaine reward by the Clock gene. Proc Natl Acad Sci USA 102:9377–9381.

McEchron MD, Bouwmeester H, Tseng W, Weiss C, Disterhoft JF (1998) Hippocampectomy disrupts auditory trace fear conditioning and contextual fear conditioning in the rat. Hippocampus 8:638–646.

Morris RG, Davis S, Butcher SP (1990) Hippocampal synaptic plasticity and NMDA receptors: a role in information storage? Philos Trans R Soc Lond B Biol Sci 329:187–204.

Peigneux P, Laureys S, Fuchs S, Collette F, Perrin F, Reggers J, Phillips C, Degueldre C, Del Fiore G, Aerts J, Luxen A, Maquet P (2004) Are spatial memories strengthened in the human hippocampus during slow wave sleep? Neuron 44:535–545.

Quinn JJ, Oommen SS, Morrison GE, Fanselow MS (2002) Post-training excitotoxic lesions of the dorsal hippocampus attenuate forward trace, backward trace, and delay fear conditioning in a temporally specific manner. Hippocampus 12:495–504.

Reppert SM, Weaver DR (2002) Coordination of circadian timing in mammals. Nature 418:935–941.

Ruby NF, Hwang CE, Wessells C, Fernandez F, Zhang P, Sapolsky R, Heller HC (2008) Hippocampal-dependent learning requires a functional circadian system. Proc Natl Acad Sci USA 105:15593–15598.

Runyan JD, Moore AN, Dash PK (2004) A role for prefrontal cortex in memory storage for trace fear conditioning. J Neurosci 24:1288–1295.

Sakai T, Tamura T, Kitamoto T, Kidokoro Y (2004) A clock gene, period, plays a key role in long-term memory formation in Drosophila. Proc Natl Acad Sci USA 101:16058–16063.

Shearman LP, Zylka MJ, Weaver DR, Kolakowski LF, Reppert SM (1997) Two period homologs: circadian expression and photic regulation in the suprachiasmatic nuclei. Neuron 19:1261–1269.

Squire LR (1992) Memory and the hippocampus: a synthesis from findings with rats, monkeys, and humans. Psychol Rev 99:195–231.

Stratmann M, Schibler U (2006) Properties, entrainment, and physiological functions of mammalian peripheral oscillators. J Biol Rhythms 21:494–506.

Toh KL, Jones CR, He Y, Eide EJ, Hinz WA, Virshup DM, Ptacek LJ, Fu YH (2001) An hPer2 phosphorylation site mutation in familial advanced sleep phase syndrome. Science 291:1040–1043.

Valentinuzzi VS, Menna-Barreto L, Xavier GF (2001) Effects of circadian phase on performance in the Morris water maze task. J Biol Rhythms 19:312–324.

Vanselow K, Vanselow JT, Westermark PO, Reischl S, Maier B, Korte T, Herrmann A, Herzel H, Schlosser A, Kramer A (2006) Differential effects of PER2 phosphorylation: molecular basis for the human familial advanced sleep phase syndrome (FASPS). Genes Dev 20:2660–2672.

Wakamatsu H, Yoshinobu Y, Aida R, Moriya T, Akiyama M, Shibata S (2001) Restricted-feeding-induced anticipatory activity rhythm is associated with a phase-shift of the expression of mPer1 and mPer2 mRNA in the cerebral cortex and hippocampus but not in the suprachiasmatic nucleus of mice. Eur J Neurosci 13:1190–1196.

Wang LM, Suthana NA, Chaudhury D, Weaver DR, Colwell CS (2005) Melatonin inhibits hippocampal long-term potentiation. Eur J Neurosci 22:2231–2237.

Welsh DK, Yoo SH, Liu AC, Takahashi JS, Kay SA (2004) Bioluminescence imaging of individual fibroblasts reveals persistent, independently phased circadian rhythms of clock gene expression. Curr Biol 14:2289–2295.

Welsh DK, Imaizumi T, Kay SA (2005) Real-time reporting of circadian-regulated gene expression by luciferase imaging in plants and mammalian cells. Methods Enzymol 393:269–288.

Whitmore D, Foulkes NS, Strahle U, Sassone-Corsi P (1998) Zebrafish Clock rhythmic expression reveals independent peripheral circadian oscillators. Nat Neurosci 1:701–707.

Wood MA, Attner MA, Oliveira AM, Brindle PK, Abel T (2006) A transcription factor-binding domain of the coactivator CBP is essential for long-term memory and the expression of specific target genes. Learn Mem 13:609–617.

Wright KP, Hull JT, Hughes RJ, Ronda JM, Czeisler CA (2006) Sleep and wakefulness out of phase with internal biological time impairs learning in humans. J Cogn Neurosci 18:508–521.

Xu Y, Toh KL, Jones CR, Shin JY, Fu YH, Ptacek LJ (2007) Modeling of a human circadian mutation yields insights into clock regulation by PER2. Cell 128:59–70.

Yamazaki S, Numano R, Abe M, Hida A, Takahashi R, Ueda M, Block GD, Sakaki Y, Menaker M, Tei H (2000) Resetting central and peripheral circadian oscillators in transgenic rats. Science 288:682–685.

Yelamanchili SV, Pendyala G, Brunk I, Darna M, Albrecht U, Ahnert-Hilger G (2006) Differential sorting of the vesicular glutamate transporter 1 into a defined vesicular pool is regulated by light signaling involving the clock gene Period2. J Biol Chem 281:15671–15679.

Yoo SH, Yamazaki S, Lowrey PL, Shimomura K, Ko CH, Buhr ED, Siepka SM, Hong HK, Oh WJ, Yoo OJ, Menaker M, Takahashi JS (2004) PERIOD2::LUCIFERASE real-time reporting of circadian dynamics reveals persistent circadian oscillations in mouse peripheral tissues. Proc Natl Acad Sci USA 101:5339–5346.

Zheng B, Larkin DW, Albrecht U, Sun ZS, Sage M, Eichele G, Lee CC, Bradley A (1999) The mPer2 gene encodes a functional component of the mammalian clock. Nature 400:169–173.

Zueger M, Urani A, Chourbaji S, Zacher C, Lipp HP, Albrecht U, Spanagel R, Wolfer DP, Gass P (2006) mPer1 and mPer2 mutant mice show regular spatial and contextual learning in standardized tests for hippocampus-dependent learning. J Neural Transmission 113:1435–1463.

ASN NEURO | RESEARCH ARTICLE

Expression of the circadian clock gene *Period2* in the hippocampus: possible implications for synaptic plasticity and learned behaviour

Louisa M–C Wang*, Joanna M Dragich*,†, Takashi Kudo*, Irene H Odom*, David K Welsh‡,§, Thomas J O'Dell‖ and Christopher S Colwell*1

*Department of Psychiatry and Biobehavioral Sciences, University of California, Los Angeles, 760 Westwood Plaza, Los Angeles, CA 90024-1759, U.S.A.
†Department of Neurology, Columbia University, New York City, NY 10032, U.S.A.
‡Departmentof Psychiatry and Cell and Developmental Biology, University of California, San Diego, La Jolla, CA 92093, U.S.A.
§Veterans Affairs San Diego Healthcare System, San Diego, CA 92161, U.S.A.
‖Department of Physiology, University of California, Los Angeles, 760 Westwood Plaza, Los Angeles, CA 90024-1759, U.S.A.

SUPPLEMENTARY DATA

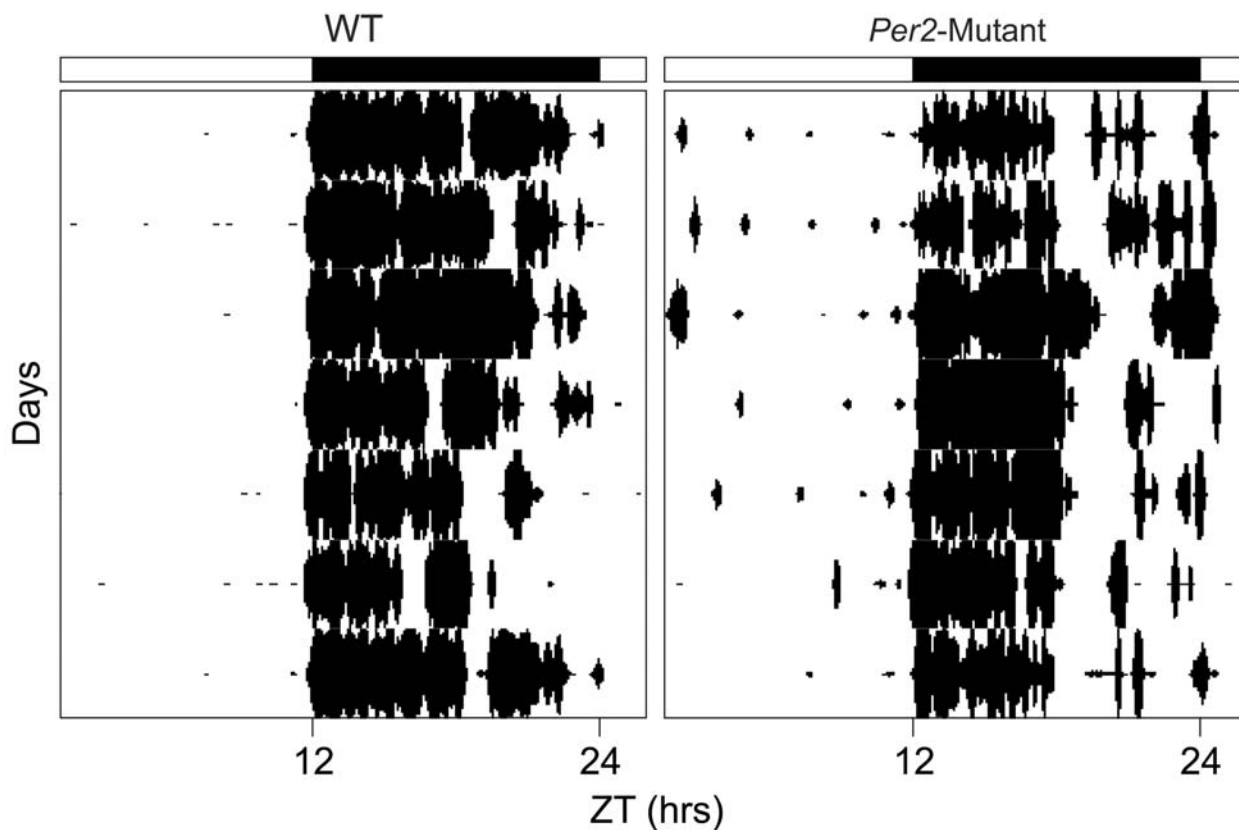[1] To whom correspondence should be addressed (email ccolwell@mednet.ucla.edu).

Figure S1   **IHC controls for the PER2 staining in the hippocampus**
(A) Photomicrographs of the hippocampus stained with the Per2 antibody taken under lower (left-hand panel, 50×, scale bar=500 µm) and higher (right-hand panel, 400×, scale bar=100 µm) power. IHC expression was largely localized to the pyramidal cell body regions within the hippocampus. (B) In the absence of the primary anti-serum, no immunopositive cells were observed. (C) When the primary anti-serum was mixed with the PER2 peptide (1 mg/ml in PBS, pH 7.4, diluted 1:500), no immunopositive cells were observed.

Figure S2   Co-localization of PER2 immunoreactivity and the nuclear staining
Photomicrographs of the CA1 layer of the hippocampus taken with a confocal microscope at high magnification (630 ×). The left-hand panel shows the staining with the PER2 antibody (1:4000 dilution). The middle panel shows staining with the nuclear marker (TO-PRO3, 1:2000 dilution). The right-hand panel shows the merged images with yellow showing the overlap in staining. There was also clear immunoreactivity that did not co-localize with the nuclear marker. We interpret this to indicate that PER2 is present in both the nucleus and cytoplasm of hippocampal cells.

Figure S3   Per2-mutant mice exhibit daily rhythms in wheel-running activity
Mice were place in cages with access to a running wheel and wheel-running activity was recorded. Examples of wheel-running activity from a WT mouse (left-hand panel) and a *Per2*-mutant mouse (right-hand panel) are shown. Bars at the top of the panels indicate the LD cycle. All of the mice evaluated exhibited daily rhythms in activity.